THE JOURNAL OF BIOLOGICAL CHEMISTRY
Vol. 279, No. 44, Issue of October 29, pp. 46295–46303, 2004
Printed in U.S.A.

Site-saturation Mutagenesis of Tyr-105 Reveals Its Importance in Substrate Stabilization and Discrimination in TEM-1 β-Lactamase*

Received for publication, July 7, 2004, and in revised form, August 17, 2004
Published, JBC Papers in Press, August 23, 2004, DOI 10.1074/jbc.M407606200

Nicolas Doucet‡, Pierre-Yves De Wals‡, and Joelle N. Pelletier‡§¶

From the ‡Département de Biochimie and §Département de chimie, Université de Montréal, C. P. 6128, Succursale Centre-ville, Montréal, Québec H3C 3J7, Canada

The conserved Class A β-lactamase active site residue Tyr-105 was substituted by saturation mutagenesis in TEM-1 β-lactamase from *Escherichia coli* in order to clarify its role in enzyme activity and in substrate stabilization and discrimination. Minimum inhibitory concentrations were calculated for *E. coli* cells harboring each Y105*X* mutant in the presence of various penicillin and cephalosporin antibiotics. We found that only aromatic residues as well as asparagine replacements conferred high *in vivo* survival rates for all substrates tested. At position 105, the small residues alanine and glycine provide weak substrate discrimination as evidenced by the difference in benzylpenicillin hydrolysis relative to cephalothin, two typical penicillin and cephalosporin antibiotics. Kinetic analyses of mutants of interest revealed that the Y105*X* replacements have a greater effect on K_m than k_{cat}, highlighting the importance of Tyr-105 in substrate recognition. Finally, by performing a short molecular dynamics study on a restricted set of Y105*X* mutants of TEM-1, we found that the strong aromatic bias observed at position 105 in Class A β-lactamases is primarily defined by a structural requirement, selecting planar residues that form a stabilizing wall to the active site. The adopted conformation of residue 105 prevents detrimental steric interactions with the substrate molecule in the active site cavity and provides a rationalization for the strong aromatic bias found in nature at this position among Class A β-lactamases.

During the past decades, β-lactamase production (EC 3.5.2.6) has become a significant problem in bacterial strain resistance to widely used clinical antibiotics. Among these enzymes, the prevalent type has always been the Class A active site serine hydrolase β-lactamases, which have become model enzymes extensively studied by protein engineering with respect to site-directed or combinatorial mutagenesis (1–5), structure determination (6–10), and molecular simulations (11–13). Over the years *Escherichia coli* TEM-1 β-lactamase has become an impressive example of the rapid evolution rate of proteins occurring within natural bacterial isolates subjected to selective pressure. Ever since the clinical introduction of β-lactam compounds and the discovery of TEM-1 β-lactamase, both in the 1940s (14), natural mutations have generated a large number of single and multiple mutants of this enzyme (for an extensive list see www.lahey.org/Studies/temtable.asp).

The high rate of occurrence of mutated enzymes capable of hydrolyzing higher generation cephalosporins has stimulated research of β-lactamase adaptation to these new substrates in order to understand the molecular basis of this evolutionary chain of events. Consequently, a number of studies have successfully predicted the *in vitro* appearance of new mutations conferring resistance before their appearance in natural isolates (for an overall view, see Ref 1). To provide more information regarding these mutations in enzyme catalysis and/or substrate stabilization, multiple mutagenesis replacements have been undertaken in Class A β-lactamases to residues in close proximity to the active site cavity that are most likely to be in direct contact with the substrate, allowing for modified catalytic parameters (2–4). In conjunction with the SDN loop (3), the Class A conserved residue Tyr-105 delineates one of the edges of the active site cavity of TEM-1 as a result of the position of its side chain near the thiazolidine ring of penicillin substrates and the dihydrothiazine ring of cephalosporin substrates. To date, two independent mutagenesis studies were performed to modify Tyr-105 to Phe and Cys on the Class A β-lactamases of *Bacillus licheniformis* and *Bacillus cereus*, respectively (15, 16). The *B. licheniformis* Y105F mutant displayed a 52% catalytic efficiency toward benzylpenicillin compared with its corresponding wild-type enzyme. Based on these results, the Y105F mutation rules out a critical role of the hydroxyl group of the wild-type Tyr residue toward enzyme activity or stability. Moreover, the *B. cereus* Y105C mutant displayed native-like catalytic activity under standard nitrocefin assay conditions, demonstrating that the aromatic moiety at this position is not essential for enzyme activity or stability.

On the other hand, the location and the strong conservation of aromatic character of this residue among Class A β-lactamases suggest that residue 105 may play a role in substrate recognition and/or stabilization. This hypothesis is based on crystallographic data of many Class A enzymes showing that the Tyr-105 side chain is significantly displaced upon binding of substrates or mechanism-based inhibitors as a result of a flipping motion (7, 17–21). In fact, it has been suggested that the Tyr-105 side chain may "stack" with the thiazolidine ring of penicillins (21, 22) as well as form van der Waals and hydrophobic interactions with the benzyl side chains of substrates (7, 12) or inhibitors (18, 19), suggestive of its active participation in substrate and inhibitor positioning at the active site. As a result of this characteristic, residue 105 has been considered a determinant of susceptibility to mechanism-based inhibitors (23).

To our knowledge, apart from the Y105F and Y105C mutations (15, 16), no further site-directed mutagenesis studies have been undertaken specifically at this critical active site position. Huang *et al.* (24) previously reported a three-codon-

* This work was supported by grants from the Natural Sciences and Engineering Research Council of Canada and the Fond Québécois de la Recherche sur la Nature et les Technologies. The costs of publication of this article were defrayed in part by the payment of page charges. This article must therefore be hereby marked "*advertisement*" in accordance with 18 U.S.C. Section 1734 solely to indicate this fact.

¶ To whom correspondence should be addressed. Tel.: 514-343-2124; Fax: 514-343-7586; E-mail: joelle.pelletier@umontreal.ca.

based combinatorial mutagenesis for the entire gene of TEM-1 but conducted no detailed analysis of residue 105 with respect to substrate recognition. Nevertheless, their results suggest that only the Y105H mutant is able to confer wild-type activity for ampicillin upon selecting for survival in the presence of 1 mg/ml antibiotic. However, these Y105*X* mutations were performed only with other simultaneous mutations at positions 103 and 104. Although the high activities observed with the Y105F and Y105C mutants suggest that hydrophobicity may be a determining factor at this active-site position, the effects of variables such as side-chain volume, polarity, and flexibility at this position have not been specifically addressed.

Thus, the importance of sequence conservation at position 105 is unclear, and the role of residue 105 has yet to be elucidated in detail with respect to enzyme stability and substrate stabilization and discrimination for Class A β-lactamases. Consequently, to clarify the importance of residue 105 in TEM-1 β-lactamase as well as its potential role in other Class A β-lactamases, we performed saturation mutagenesis at position 105 on TEM-1. *In vivo* antibiotic susceptibility tests and *in vitro* kinetic studies were carried out using penicillin as well as first- and third-generation cephalosporin substrates to assess the impact of the mutations on substrate recognition and enzyme catalysis. Finally, molecular modeling studies of mutants of interest were undertaken to evaluate the structural importance of residue 105 in substrate stabilization. Our results identify residue 105 as a weak substrate determinant of TEM-1 β-lactamase.

EXPERIMENTAL PROCEDURES

Reagents—Restriction and DNA-modifying enzymes were purchased from MBI Fermentas (Burlington, ON) and New England Biolabs, Ltd. (Mississauga, ON). Ampicillin was obtained from BioShop Canada, Inc. (Burlington, ON), and benzylpenicillin, cephalothin, cefazolin, cefotaxime, and Fast-Flow DEAE-Sepharose were purchased from Sigma-Aldrich. Nitrocefin was purchased from Calbiochem.

Bacterial Strains and Plasmids—*E. coli* XL1-Blue (*supE44*, *hsdR17*, *recA1*, *endA1*, *gyrA46*, *thi*, *relA1*, *lac* F′ [*proAB*$^+$, *lacI*^{q}, *lacZΔM15*, Tn*10*(*tet*^{r})]) was used for the propagation and expression of all plasmids. Plasmid pQE32Chl in which the bla_{TEM-1} gene of pQE32 (Qiagen, Mississauga, ON) was replaced by a chloramphenicol acetyltransferase gene was a generous gift from François-Xavier Campbell-Valois and Stephen W. Michnick (Département de Biochimie, Université de Montréal, QC) and was used for protein expression. It was maintained using 12.5 μg/ml chloramphenicol (Chl).[1] Plasmid pBR322, which contains the wild-type bla_{TEM-1} gene (without the V84I and A184V mutations) was kindly provided by Luis A. Rokeach (Département de Biochimie, Université de Montréal, QC).

Oligonucleotides and Saturation Mutagenesis—Oligonucleotide primers used for mutagenesis were synthesized by Alpha DNA (Montréal, QC) and Integrated DNA Technologies (Coralville, IA). Oligonucleotide primers used for DNA sequencing were synthesized by Li-Cor Biotechnology (Lincoln, NB). The Y105*X* mutants of TEM-1 were constructed using the site overlap extension mutagenesis method (25). The 861-bp bla_{TEM-1} gene was PCR-amplified from plasmid pBR322 using the terminal oligonucleotides BamHITEMF (5′-CACACAGGATCCACATGAGTATTCAACATTTCCGT-3′) and TEMHindIIIR (5′-ACACACAAGCTTTTACCAATGCTTAATCAGTGA-3′) containing the BamHI and HindIII restriction sites (underlined), respectively. The 19-amino acid possibilities at codon 105 were introduced by a set of three complementary pairs of degenerate oligonucleotides (only the coding strands are shown): TEM105NTSF (5′-ATGACTTGGTTGAGNTSTCACCAGTCACAG-3′), TEM105NGSF (5′-ATGACTTGGTTGAGNGSTCACCAGTCACAG-3′), and VMS105F (5′-ATGACTTGGTTGAGVMSTCACCAGTCACAG-3′). The use of three separate degenerate oligonucleotides encoding the possibilities NTS, NGS, and VMS instead of a single NNS codon was justified by the elimination of the wild-type tyrosine residue as well as the three stop codons.

The recombinant TEM genes were digested with BamHI/HindIII and cloned into BamHI/HindIII-digested and calf intestinal alkaline phosphatase-treated pQE32Chl before electroporation into *E. coli* XL1-Blue cells. Colonies were individually picked after selection on a Luria-Bertani (LB) medium containing 12.5 μg/ml Chl, and the sequence of each mutant was confirmed by the dideoxy chain termination method with the Thermo Sequenase Cycle Sequencing kit (Upstate Biotechnology Corp., Cleveland, OH) using a dye-labeled primer and a Li-Cor automated sequencer (Lincoln, NB).

Expression and Purification of Mutant β-Lactamases—An overnight culture of each XL1-Blue/pQE32Chl-TEM(Y105*X*) clone was used to inoculate 50 ml of LB that was grown with agitation at 37 °C until $A_{600\ nm}$ = 0.6. After the addition of 1 mM isopropyl 1-thio-β-D-galactopyranoside, the cultures were propagated for an additional 3 h. After induction, the cells were pelleted by centrifugation (30 min, 3000 × *g*, 4 °C), resuspended in 10 ml of 10 mM Tris-Cl buffer, pH 7.0, and separated in 1-ml aliquots. A gentle lysis of the outer membrane of *E. coli* was performed by 3–4 1.5-min freeze-thaw cycles using a dry-ice/ethanol and a 37 °C water bath followed by a centrifugation (15 min, 20,000 × *g*, 4 °C) to collect the supernatant.

Purification of TEM(Y105*X*) mutants of interest was performed according to the following single-step anion-exchange chromatography procedure. All steps were undertaken at 4 °C with a flow rate of 1 ml/min on a System Gold high performance liquid chromatography apparatus (Beckman Coulter Canada, Inc., Mississauga, ON). Supernatant (10 ml) was applied to a DEAE-Sepharose column (2 × 25 cm) followed by a wash of 2.5 column volumes with 10 mM Tris-Cl, pH 7.0, buffer. Mutant enzymes were eluted with a linear gradient of 10–150 mM Tris-Cl, pH 7.0, buffer (1.5 column volume), and a subsequent wash with the same buffer was finally performed (2.5 column volumes). Fractions containing β-lactamase activity were identified by a qualitative nitrocefin hydrolysis test and pooled for subsequent analysis. Aliquots of each clone were analyzed by SDS-PAGE gel, and the purity was estimated in all cases to be between 80 and 90% using the public domain image analysis software Scion Image (National Institutes of Health, rsb.info.nih.gov/nih-image). The column was regenerated by applying 5 volumes of 8 M urea followed by 5 volumes of 10 mM Tris-Cl, pH 7.0, buffer between each purification. No significant β-lactamase activity carryover was detected by nitrocefin assay upon running a mock purification (cells expressing no TEM-1 β-lactamase) following a purification of the native TEM-1.

Antibiotic Susceptibility—Minimum inhibitory concentrations (MICs) were determined by broth microdilutions according to Cantu *et al.* (26). The ranges of antibiotic concentrations tested were as follows (by stepwise 2-fold increases): 125–4000 μg/ml for benzylpenicillin and ampicillin, 4–500 μg/ml for cephalothin, 1–125 μg/ml for cefazolin, and 4–500 ng/ml for cefotaxime. Each MIC determination was performed at least in triplicate in independent experiments.

Enzyme Kinetics—The kinetic constants K_m and k_{cat} for benzylpenicillin and cephalothin were determined at room temperature in 50 mM sodium phosphate buffer, pH 7.0, for the mutants presented in Table III. The following extinction coefficients (27) and concentration ranges were used: $\Delta\epsilon_{232\ nm}$ = 1100 M^{-1} cm^{-1} for benzylpenicillin (50–200 μM) and $\Delta\epsilon_{262\ nm}$ = 7960 M^{-1} cm^{-1} for cephalothin (30–300 μM). Substrate hydrolysis was monitored according to initial steady-state velocities for a minimum of six substrate concentrations generally flanking the K_m values (when the molar extinction coefficients and the K_m value allowed it) using a Cary 100 Bio UV-visible spectrophotometer (Varian Canada, Inc., Montréal, QC). For each assay the concentration of enzyme was kept at least 500 times lower than substrate for benzylpenicillin (BZ) and was generally 50 times lower for cephalothin (CF). The kinetic parameters were determined from the rates of hydrolysis calculated from the initial linear portion of the curve and fitted to a Lineweaver-Burk (1/[S] *versus* 1/[V]) and a Hanes ([S] *versus* [S]/*V*) plot. In most cases initial rates were also analyzed with the software Graphpad Prism (Graphpad Software, San Diego, CA) by a non-linear regression curve corresponding to the Michaelis-Menten equation. The k_{cat} parameter was determined using the equation $k_{cat} = V_{max}/[E]$, where the concentration of enzyme was determined by a Bio-Rad protein assay kit (Bio-Rad) taking into account its purity, estimated as described above.

Computer Modeling—All computations were performed with the InsightII package, version 2000 (Accelrys, San Diego, CA). The BIOPOLYMER module was used to modify molecular structures, and all energy minimizations and molecular dynamics calculations were performed with the DISCOVER module using the consistent valence force field. The dynamic trajectories were analyzed using the DECIPHER module. We performed the simulations with the coordinates of an acyl-enzyme intermediate of TEM-1 complexed with benzylpenicillin

[1] The abbreviations used are: Chl, chloramphenicol; AMP, ampicillin; BZ, benzylpenicillin; CF, cephalothin; CZ, cefazolin; MIC, minimum inhibitory concentration.

(BZ), and we created an acyl-enzyme model of TEM-1 complexed with CF to compare the behavior of this substrate with that observed for BZ over the course of a 200-ps dynamics. We also conducted molecular dynamics studies using the coordinates of an apoenzyme structure of TEM-1 with residue 105 mutated, to assess conformation before substrate binding. Comparison of these systems (BZ acyl-enzyme, CF acyl-enzyme, and apoenzyme) allowed for the evaluation of the conformation of residue 105 before and after substrate recognition.

The 1.8-Å crystallographic structure of the *E. coli* TEM-1 β-lactamase (Protein Data Bank, Brookhaven National Laboratory, code 1BTL) (28) was used for the starting coordinates for apoenzyme calculations, and the 1.7-Å crystallographic structure of a E166N deacylation-defective mutant of the same enzyme (PDB code 1FQG) (8) was used for the starting coordinates for calculations involving benzylpenicillin-bound enzyme. The crystallographic water molecules of both enzymes were conserved. The active site SO_4 molecule was deleted from 1BTL, and the E166N mutation of 1FQG was reverted to wild type. Hydrogen atoms were added at the normal ionization state of the amino acids at pH 7.0. For 1FQG, the atomic potentials of the BZ substrate were fixed according to the consistent valence force field atom types recommended by the manufacturer. These coordinates served as the starting points for all the subsequent calculations in presence (1FQG) or absence (1BTL) of BZ.

The Y105G, Y105L, Y105N, Y105Q, Y105R, and Y105W mutations were introduced. Before minimization, the tryptophan side chain was repositioned according to the crystal structure of the structurally homologous Class A PER-1 β-lactamase (PDB code 1E25) (9). Residues contained in a simulation area within 15 Å from any atom of BZ (1FQG) or residue 105 (1BTL) were allowed to move as well as the loop encompassing residues 96–116, with the remainder of the protein being fixed. A layer of 5 Å of explicit water was added to the surface of this assembly, and a nonbonded cutoff of 20 Å was fixed to reduce the time of calculation. Each structure was energy-minimized by applying 100 steps of steepest descents followed by a conjugate gradient minimization until convergence of 0.001 kcal mol^{-1} $Å^{-1}$. A short molecular dynamics simulation was performed starting from the energy-minimized structures. Accordingly, the molecular system was allowed to equilibrate at 310 K for 100 fs followed by the actual simulation to explore conformational space for 200 ps at the same temperature (time step = 1 fs). Snapshots were taken each picosecond, generating 201 different conformers. At this point the trajectories obtained for each mutant were analyzed.

To create the acyl-enzyme intermediate models of TEM-1 with cephalothin (TEM-CF and Y105G-CF), the atomic coordinates of CF were taken from the crystal structure of an acyl-enzyme intermediate of TOHO-1 β-lactamase (PDB code 1IYP) (10) and fitted to the 1.8-Å crystallographic structure of the *E. coli* TEM-1 β-lactamase (PDB code 1BTL). The active site SO_4 molecule was deleted from 1BTL, and the CF substrate was positioned according to BZ in 1FQG by applying torsions to the Cβ-Oγ bond of Ser-70. Hydrogen atoms were adjusted to pH 7, and the atomic potentials of CF were adjusted as described herein. An energy minimization was performed on this structure by applying 100 steps of steepest descents followed by a conjugate gradient minimization until convergence of 0.001 kcal $mol^{-1}Å^{-1}$. This structure served as the starting coordinate for all subsequent steps of minimization and dynamics studies, which were performed as described above.

RESULTS

Antibiotic Susceptibility—We mutated position 105 (Tyr) of TEM-1 β-lactamase to the 19 other possibilities and confirmed through DNA sequencing of the entire gene that no secondary mutations had occurred. To assess the effect of the Y105*X* replacements on the capacity of TEM-1 to hydrolyze penicillin-type and cephalosporin antibiotics, MICs were calculated for *E. coli* XL1-Blue cells alone or expressing TEM-1 mutants. The antibiotics used are presented in Fig. 1. Table I presents MIC values determined for all mutants toward two classical penicillin-type substrates, BZ and ampicillin (AMP) as well as two typical first-generation cephalosporins, cephalothin (CF) and cefazolin (CZ). Thus, *in vivo* cell survival at higher antibiotic concentrations reflects a higher rate of hydrolysis by the enzyme. Because they are performed *in vivo*, MIC values serve as points of comparison rather than precise values and do not directly correlate with the K_m or k_{cat} parameters of each mutant enzyme. They nevertheless offer a rapid, qualitative assessment of the efficiency of mutants and allow for the identification of mutants deemed to be the most interesting with respect to detailed kinetic analysis.

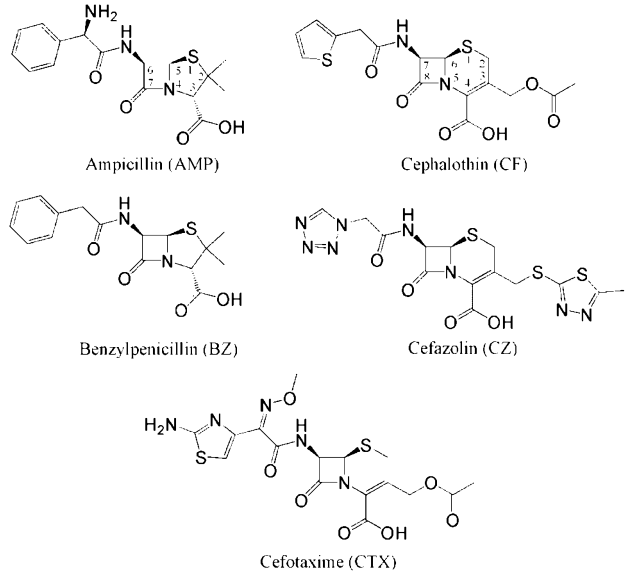

FIG. 1. **Structures of β-lactam antibiotics used in this study.** Ampicillin and benzylpenicillin are classical penicillins, whereas cephalothin and cefazolin are first-generation cephalosporins. Cefotaxime is a third-generation cephalosporin.

As seen in Table I, the range of resistance is higher for the penicillin substrates (500–4000 μg/ml for BZ and 500–7500 μg/ml for AMP) than for the cephalosporin substrates (16–125 μg/ml for CF and 4–250 μg/ml for CZ). This result was expected since Class A β-lactamases hydrolyze penicillins much more efficiently than cephalosporins, the latter having been historically developed to counteract the appearance of natural resistance to penicillins (29, 30). Nonetheless, the 20 mutants allow for a comparable breadth of resistance with respect to these four substrates. Thus, the ratio between the least and the most active mutants for BZ hydrolysis is approximately one order of magnitude (500 μg/ml relative to 4000 μg/ml), similar to that observed for CF hydrolysis (16 μg/ml relative to 125 μg/ml). AMP and CZ allow for slightly broader ranges but remain in the same range of resistance as BZ and CF, respectively.

This breadth of resistance illustrates that position 105 replacements can alter enzyme efficiency up to a factor of 10-fold. Nonetheless, this relatively weak effect confirms previous observations suggesting that position 105 cannot be considered essential for enzyme catalysis in Class A β-lactamases (15, 31). To understand the source of the effect, we examined the following hypotheses; (*a*) disparity in enzyme solubility conferred by the Y105*X* replacements, (*b*) changes in periplasmic localization efficiency of some Y105*X* mutants, (*c*) an active site cavity disruption modifying substrate recognition or catalytic turnover. We verified that the mutations at position 105 have little effect on solubility and on periplasmic localization by quantifying the soluble expression levels for each Y105*X* mutant after outer-membrane lysis. The soluble, periplasmic β-lactamase concentration observed by SDS-PAGE for all Y105*X* mutants was within a factor of 2 relative to the wild-type enzyme. The small variations observed did not correlate with the MIC results and are most likely slight clonal variations (data not shown). This result indicates that the mutations at position 105 do not significantly affect solubility or periplasmic localization, suggesting little impact on enzyme structure. This observation is consistent with previous results of circular dichroism studies on the Y105F mutant of the Class A β-lacta-

TABLE I
MICs of E. coli XL1-Blue cells expressing TEM-1 β-lactamase with Tyr-105 replacements

MIC (μg/ml)	Benzylpenicillin (BZ) Amino Acid 105[a]	Ampicillin (AMP) Amino Acid 105
7500		A
4000	A, F, G, H, *N*, W, Y	F, *N*, W, Y
2000	C, K, M, P, *Q*, S	C, D, G, H, K, L, P, *Q*, S, T, V
1000	E, I, L, R, T, V	E, I, M
500	D	R
125	None[b]	None

MIC (μg/ml)	Cephalothin (CF) Amino Acid 105	Cefazolin (CZ) Amino Acid 105
250		W
125	W, Y	
63	F, H, *N*	H, Y
32	D, M, P	F, *N*
16	A, C, E, G, I, K, L, *Q*, R, S, T, V, None	G, P
8		A, C, E, I, K, M, *Q*, R, S, T, V
4		D, L, None

[a] Aromatic residues are boxed in bold, and charged residues are boxed in white. Residues Asn and Gln are in italics, and Ala and Gly are underlined.
[b] *E. coli* XL1-Blue.

mase of *B. licheniformis* (15). Thus, these results imply that the Y105*X* replacements have an effect on substrate recognition and/or turnover in the active site of TEM-1.

A considerable number of mutants confer antibiotic resistance in the same range (or higher) as the wild-type enzyme for all of the substrates tested. This provides confirmation that position 105 does not need to be strictly conserved for enzyme activity and suggests that the observed differences in activity may result from a structural disturbance within the active site cleft that alters substrate recognition. It is striking to note that only aromatic replacements as well as Asn and the small residues Ala and Gly in some cases allow for survival rates in the same antibiotic concentration range as the wild-type enzyme for the four substrates tested. Notwithstanding a general similarity in the effects of the mutations toward penicillin-type and cephalosporin substrates, important differences were observed. Thus, Table I shows that all Y105*X* mutants confer at least a minimal resistance to BZ and AMP, which is not the case for CF and CZ. For instance, the lowest MIC recorded for BZ (Y105D) still confers a resistance to this antibiotic at least four times higher than the *E. coli* cells alone. On the contrary the majority of Y105*X* mutants were unable to confer any survival over background in the presence of CF or conferred at most a 2-fold higher MIC than background toward CZ. These results demonstrate that the Y105*X* replacements are more deleterious toward turnover of the cephalosporin substrates than they are for the penicillin counterparts.

All except one of the highly active Y105*X* mutations (Ala) are found at the corresponding position in other natural Class A β-lactamases, which have a strong preference for aromatic residues, although Asn and Gly have also been identified to date (Table II). Accordingly, the Y105*X* mutants show a high *in vivo* antibiotic resistance bias for aromatic residues as well as Asn at position 105 for all the substrates tested. The occurrence of Asn and two small, non-polar residues (Ala and Gly) among the most highly BZ- and AMP-resistant mutants confirms that aromatic residues are not essential for hydrolysis of penicillins. This relation is not so clear in the case of cephalosporin resistance, where the Ala and Gly mutants are in the lower portion of the resistance spectrum for CF and CZ, suggesting that the identity of the residue at position 105 may participate in ligand selectivity.

TABLE II
Sequence alignment of residues 103–107 for major representatives of Class-A β-lactamase
Data were compiled from previously published reports (9, 40).

Enzyme	Residue number[a]				
	103	104	105	106	107
TEM-1	Val	Glu	Tyr	Ser	Pro
SHV-1	Val	Asp	Tyr	Ser	Pro
TOHO-1	Val	Asn	Tyr	Asn	Pro
PC-1	Val	Ala	Tyr	Ser	Pro
PSE-4	Val	Thr	Tyr	Ser	Pro
P. aeruginosa	Val	Thr	Tyr	Ser	Pro
Staphylococcus aureus	Val	Ala	Tyr	Ser	Pro
B. licheniformis	Val	Asn	Tyr	Asn	Pro
B. cereus III	Ser	Asn	Tyr	Asn	Pro
PER-1[b]	Leu	Thr	Trp	Ala	Pro
VEB-1[b]	Leu	Thr	Trp	Ser	Pro
Klebsiella oxytoca	Val	Val	Trp	Ser	Pro
CME-1[b]	Leu	Thr	Trp	Ser	Pro
NMC-A	Glu	Phe	His	Ser	Pro
IMI-1	Glu	Phe	His	Ser	Pro
SME-1	Glu	Tyr	His	Ser	Pro
M. fortuitum	Val	Pro	Asn	Ser	Pro
*Stroptonyces cacaoi bla*U	Val	Asp	Asn	Ser	Pro
S. albus G	Glu	Asp	Gly	Ala	Pro
Stroptonyces lavendulae			Phe	Gly	Pro

[a] Residue numbering according to Ambler *et al.* (40).
[b] These β-lactamases harbor a three-residue insertion between positions 103 and 104.

For BZ and AMP recognition, no charged mutant (Lys, Arg, Asp, and Glu) allowed for cell growth at concentrations greater than half that displayed by the native enzyme, whereas for CF and CZ, these mutants conferred a resistance to concentrations 4 and 8 times lower than the parental enzyme, respectively. These results suggest that aromatic residues as well as Asn at position 105 participate in substrate recognition or turnover, perhaps by providing favorable interactions with the substrate, whereas in the case of other residues at position 105 the interactions would be detrimental or simply absent.

To characterize the impact of Y105*X* mutations toward rec-

TABLE III
Kinetic parameters for wild-type TEM-1 β-lactamase and Y105X mutant derivatives

Substrate	TEM-1 variant	k_{cat}	k_{cat} relative to wild type	K_m	K_m relative to wild type	k_{cat}/K_m	k_{cat}/K_m relative to wild type
		s^{-1}		μM		$M^{-1}\ s^{-1}$	
BZ	Wild type	1240 ± 125	1.00	43 ± 9	1.00	2.9×10^7	1.00
	Y105D	255 ± 20	0.21	369 ± 23	8.58	6.9×10^5	0.02
	Y105G	1203 ± 350	0.97	152 ± 61	3.53	7.9×10^6	0.27
	Y105N	1616 ± 339	1.30	276 ± 84	6.42	5.9×10^6	0.20
	Y105R	525 ± 70	0.42	156 ± 38	3.62	3.4×10^6	0.12
	Y105W	900 ± 78	0.73	23 ± 9	0.53	3.9×10^7	1.34
CF	Wild type	105 ± 11	1.00	177 ± 27	1.00	5.9×10^5	1.00
	Y105D	51 ± 11	0.49	2860 ± 540	16.2	1.8×10^4	0.03
	Y105G	45 ± 18	0.43	1630 ± 750	9.21	2.8×10^4	0.05
	Y105N	61 ± 17	0.58	303 ± 97	1.71	2.0×10^5	0.34
	Y105R	90 ± 28	0.86	546 ± 34	3.08	1.6×10^5	0.27
	Y105W	65 ± 8	0.62	74 ± 22	0.42	8.8×10^5	1.49

ognition of higher generation cephalosporins, MIC values were also determined for cefotaxime, a third generation cephalosporin substrate that is not efficiently recognized by wild-type TEM-1 (2). No cell survival above background for *E. coli* XL1-Blue cells was observed for the parental enzyme or for any Y105*X* mutant (results not shown).

Enzyme Kinetics—The MIC values for various antibiotics allowed us to identify specific Y105*X* mutants of interest for further enzymatic characterization, notably the Trp, Asn, Gly, Arg, and Asp mutants. Trp was chosen because of its aromatic similarity with the native Tyr, its high *in vivo* activity, and also because of its frequent occurrence in other Class A β-lactamases (Table II). Asn was chosen because its side chain is non-aromatic and much smaller while still being a highly active mutant also occasionally represented in other Class A β-lactamases. To our knowledge Gly has been identified in one Class A β-lactamase (Table II) and was selected because, like Ala, its *in vivo* behavior is different toward penicillins and cephalosporins. Finally, Asp and Arg are two charged residues that were chosen because of their low *in vivo* activity. Neither of the latter residues has been identified at position 105 in Class A β-lactamases. We performed the *in vitro* assays using BZ and CF as representatives of the penicillin and first generation cephalosporin substrate classes, respectively.

The steady-state kinetic parameters for native TEM-1 and the five selected mutants were calculated for BZ and CF (Table III). The greater catalytic efficiency (k_{cat}/K_m) of the wild-type TEM-1 for BZ is attributed to a 4-fold decrease in K_m and a 12-fold increase in k_{cat} toward BZ hydrolysis relative to CF. The most active mutant tested (Y105W) has a catalytic efficiency in the same range as the native enzyme, whereas the least active one (Y105D) displays a reduction of 2 orders of magnitude in its catalytic efficiency with respect to both substrates. Although both Y105G and Y105N have catalytic efficiencies 3–5 times lower than the wild-type enzyme for BZ, their kinetic properties with respect to CF hydrolysis are not alike. Indeed, although Y105N is 3-fold less efficient than the wild-type enzyme, the efficiency of Y105G drops to a value that is 20-fold lower for CF hydrolysis as a result of a significant K_m increase. The different effect of the Y105G mutation on K_m values for the two antibiotics indicates that the Y105G mutant behaves in a different manner with respect to penicillin and cephalosporin recognition, confirming the trend that was observed in the MIC determinations.

In general, the deleterious effects of many of the Y105*X* mutations on catalytic efficiency is the result of a greater disruption of K_m than k_{cat}, although this trend is more pronounced for CF hydrolysis than for BZ. The greatest k_{cat} decreases observed were for BZ hydrolysis for the Y105R and Y105D mutants, which display a turnover number (k_{cat}) ~2.5 and 5 times lower than the parental enzyme, respectively. However, Y105G, Y105N, and Y105W hydrolyze the penicillin at maximal rates ±30% relative to the native enzyme. With respect to K_m, the most active mutant (Y105W) shows a 2-fold decrease in K_m compared with the parental enzyme. Other mutants show important K_m increases that range from 3.5-fold (Y105G and Y105R) to 8.6-fold differences (Y105D). These combined effects on k_{cat} and K_m result in catalytic efficiencies for BZ hydrolysis that range between 20 and 130% of wild-type TEM-1 for mutants Y105G, Y105N, and Y105W, which showed native-like BZ MICs, whereas Y105R (12%) and Y105D (2%) are also less efficient *in vivo* (Table I). These results indicate that position 105 mutants displaying a catalytic efficiency approximately one-fifth or higher than that of the wild-type enzyme (Y105G, Y105N, Y105W) confer *in vivo* survival rates in the same range as the wild-type parent for BZ hydrolysis, whereas those with lower efficiency (Y105R, Y105D) result in poor *in vivo* performance. Thus, the K_m of Y105R may define a threshold below which there is enough productive binding *in vivo* to guarantee drug resistance.

Although the five characterized mutants hydrolyze CF with a k_{cat} that remains within 50–100% of the wild-type enzyme, K_m is modified much more importantly. As with BZ, the most active mutant (Y105W) shows a 2-fold decrease in K_m compared with the parental enzyme for CF hydrolysis. However, the other mutants show K_m increases ranging from 1.7 (Y105N)- to 16.2 (Y105D)-fold higher than the wild-type enzyme. K_m differences are, thus, the greatest contributor to the differences seen in the catalytic efficiency of every mutant tested for CF hydrolysis, confirming the implication of Tyr-105 in CF recognition by TEM-1 β-lactamase.

Moreover, the comparison of k_{cat} and K_m of the best and the worst mutants toward CF and BZ hydrolysis demonstrates the importance of residue 105 with respect to affinity as opposed to catalysis. In fact, although k_{cat} differs by 4.9-fold for BZ and 2.3-fold for CF when comparing the best and the worst mutants with respect to k_{cat} (wild-type/Y105D for BZ, wild-type/Y105G for CF), the comparison of K_m values yields differences of 16-fold for BZ and 39-fold for CF (Y105D/Y105W for BZ and CF). These observations lend further support to previously published results describing the Y105F mutant of the *B. licheniformis* β-lactamase, which suggested that the main effect on activity was on substrate binding as a result of a 3–4-fold increase in K_m (15). Although K_m for BZ hydrolysis does not vary as much as for CF hydrolysis, k_{cat} is affected to a somewhat greater extent for less active mutants. These differences suggest that residue 105 may be a weak substrate determinant in TEM-1, participating in substrate stabilization and providing an element of selectivity in the recognition of penicillins and cephalosporins. To further in-

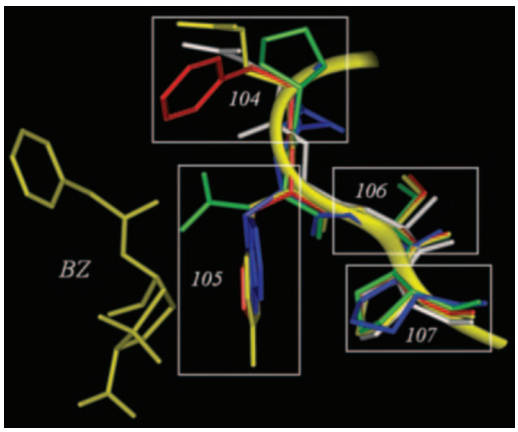

FIG. 2. **Superimposition of residues 104–107 of 5 Class A β-lactamases crystal structures.** The following enzymes were used with the corresponding PDB entries; *blue*, *Pseudomonas aeruginosa* PER-1 apoenzyme (1E25) (9); *green*, *M. fortuitum* apoenzyme (1MFO); *white*, *S. albus G* apoenzyme (1BSG) (38); *red*, *Enterobacter cloacae* NMC-A apoenzyme (1BUE) (39); *yellow*, *E. coli* TEM-1 complexed with BZ (1FQG) (8). The structural alignment was undertaken using the backbone atoms of residues 104–107 with InsightII. Main chain atoms between residues 103–108 of TEM-1 are represented as a *yellow ribbon*.

vestigate the *in vivo* and *in vitro* results obtained with BZ and CF as representatives of the penicillin and cephalosporin substrate classes, molecular dynamics studies were undertaken with selected TEM-1 β-lactamase mutants in the presence and in the absence of these substrates.

Computational Models—Tyrosine 105 is a solvent-exposed active site residue with a side-chain conformation that is structurally conserved among almost all Class A β-lactamases of known structure. Fig. 2 shows the superimposition of residues 104–107 of the crystal structures of five Class A β-lactamases found in natural isolates harboring different residues at position 105 (Tyr, Trp, His, Asn, and Gly). Of these five structures only TEM-1 is complexed with a substrate molecule (BZ). In all cases, this 104–107-residue area defines one of the walls in contact with the substrate and constitutes the turn within a relatively rigid loop-helix motif encompassing residues 96–116. Although the side chain of residue 104 is quite flexible, residues 106 and 107 have a structurally conserved conformation, as does position 105, unless it is an Asn. In all cases the side chain of residue 106 points toward the interior of the 96–116 loop-motif as a result of the sequence-conserved Pro107 (Table II) creating a characteristic distorted Type-I β-turn in the structure (23, 24, 28). When the residue at position 105 is aromatic, it always lines up in an edge-to-face manner against Pro-107 (Fig. 2). However, Asn-105 of the *Mycobacterium fortuitum* enzyme points away from the motif directly toward the active site cavity. Despite the absence of a side chain in the *Streptomyces albus G* enzyme (which harbors Gly at position 105), it is interesting to note that the turn is conserved and that the shape of the 104–107 element is unaltered. This suggests that the identity of the residue at position 105 does not determine or greatly influence this helix-loop conformational bend. The structural homology in these natural β-lactamases with varying residues at position 105 is consistent with our observation that Y105*X* mutations did not have drastic effects on TEM-1 structure, as evidenced both by conservation of the protein solubility and by retention of at least a fraction of substrate recognition and catalytic capacity. Consequently, we performed molecular dynamics simulations of the Y105*X* mutations in TEM-1, assuming that no gross structural changes had occurred.

The Trp, Asn, Gly, Arg, Gln, and Leu mutants of TEM-1 in the presence of BZ were studied for the following reasons; Trp, as a positive control for highly active, aromatic residues; Asn, because of its native-like activity despite its small, non-aromatic side chain; Gly (with BZ and CF), because of its different kinetic behavior toward those substrates despite the lack of a side chain; Arg, as a weakly active mutant with a bulky and charged side chain; Gln, as a weakly active mutant structurally similar to the highly active Asn; and finally Leu, as a weakly active mutant with a neutral and branched side chain. In all models the backbone of the entire 96–116 loop-motif displayed little motion during the 200-ps dynamics simulation (root mean square deviation <0.86 Å). Throughout the dynamics, Tyr-105 is rigidly positioned in the center of an ~8-Å-wide cavity between Pro-107 and the substrate molecule in a manner that is quite similar to the crystallographically determined conformation of other position 105 aromatic residues in Class A β-lactamases (Fig. 2). The BZ substrate also shows little motion relative to the crystal structure (root mean square deviation ≤ 1 Å). Previous studies suggest that this precise positioning of the aromatic moiety of Tyr-105 allows it to stack between Pro-107 and the thiazolidine ring of the substrate, although the nature of the proposed interaction has not been described in detail (21, 22). Our modeling results show that the distances maintained between the phenol ring of Tyr-105 and the thiazolidine ring on one side and Pro-107 on the other (~3.5 Å on both sides) and the nature of the proximal atoms are consistent with van der Waals interactions. Furthermore, no significant difference was observed in the free-form model of TEM-1 regarding rigidity or conformation of Tyr-105 (not shown).

Thus, the aromatic side chain of Tyr-105 forms a "wall" preventing the thiazolidine ring of BZ from moving into the small cavity facing Pro107 (Fig. 3*A*). The Trp mutation (Fig. 3*A*) behaves in the same manner as the wild-type enzyme, which is consistent with the native-like *in vivo* and *in vitro* activities observed for the Y105W mutant and is also consistent with high productive binding reflected by low K_m values (2-fold decrease for CF and BZ). Although the side chain of Asn is considerably smaller than the aromatic residues, the Y105N mutation appears to behave in a very homologous manner, positioning the planar, structurally constrained γ-amide group parallel to the conformation adopted by the modeled aromatic side-chains Tyr and Trp (Fig. 3*A*). This again forms a wall in front of Pro-107, preventing the substrate from moving from its original position toward Pro-107, consistent with the high survival rates observed in the MIC determinations for the Y105N mutant.

In contrast with those mutations, the Y105G replacement leaves the active site cavity considerably more open (Fig. 4). Over the course of the 200-ps trajectory, the thiazolidine ring of BZ fills the cavity facing Pro-107, where it remains relatively rigid once placed in this alternate position. Accordingly, k_{cat} is unaffected, whereas K_m increases by a factor of 3.5-fold. Nevertheless, these modifications have virtually no impact on the survival rate of this mutant with respect to BZ hydrolysis. On the other hand, CF recognition is more strongly affected by the mutation to glycine, as can be seen by the 9.2-fold increase in K_m coupled to a 2-fold drop in k_{cat}, which correlates with the low survival rates conferred by the Y105G mutant with respect to CF hydrolysis. To better characterize the *in vivo* and *in vitro* differences observed for BZ and CF with the Y105G mutant, we performed molecular dynamics studies with a TEM-1 model complexed with CF for the wild-type enzyme (Tyr-105) and for Y105G (not shown). Although we observe subtle differences in the positioning of CF relative to BZ, our models do not offer a clear explanation for the high substrate discrimination conferred by the Y105G mutant with respect to BZ and CF.

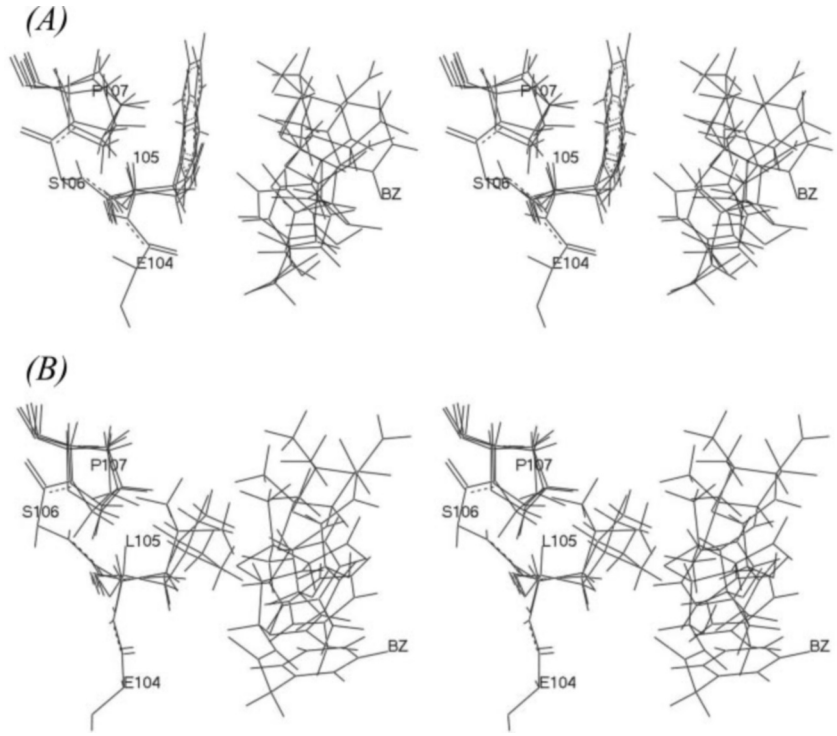

FIG. 3. **Superimpositions of snapshots from a 200-ps molecular dynamics simulation of various Y105*X* mutants of TEM-1, shown in stereo.** *A*, superimposition of residues 105 and 107 for the 200-ps snapshot of wild-type TEM-1 and mutants Y105W and Y105N. Although only the 200-ps snapshot is shown for each of the three mutants, the side chains of residues Tyr, Trp, and Asn are all in the same plane, rigidly positioned in the center of an ~8-Å-wide cavity between Pro-107 and the substrate molecule (BZ) throughout the entire 200-ps dynamics simulations. *B*, superimposition of residues 105 and 107 for the 80-, 120-, and 160-ps snapshots of mutant Y105L. The increased flexibility of the branched side chain of Leu-105 prevents adoption of the physical barrier shown in *panel A*, resulting in substrate destabilization at the active site. For both *A* and *B* representations, only residues 104–107 and the BZ substrate are shown. For clarity, the side chains of residues 104 and 106 are omitted.

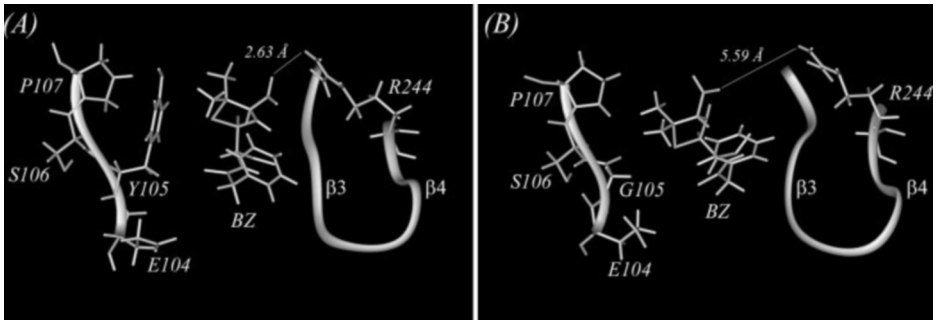

FIG. 4. **Conformation of benzylpenicillin in the active site of wild-type TEM-1 (*A*) and mutant Y105G (*B*) at the end of a 200-ps dynamics trajectory.** The shortest distance between the C3-carboxylate moiety of the thiazolidine ring of BZ to the guanidinium moiety of Arg-244 is represented. The Y105G mutation results in removal of the wall created by Tyr-105, shifting the thiazolidine ring of the substrate in the direction of Pro-107. This resulting conformation of BZ prevents direct contact of the C3-carboxylate with Arg-244 in the Y105G mutant. Backbone direction between residues 104–107 and 235–245 is represented by a *ribbon* and is shown in the same orientation as in Fig. 3. Residues from β-strands 3 and 4 (except Arg-244) are omitted for clarity. Similar results were observed with CF.

Most other residue replacements at position 105 had a detrimental effect on TEM-1 activity toward both penicillins and cephalosporins. After a 200-ps dynamics simulation performed with BZ for Arg or Gln at position 105, we observed large differences relative to position 105 mutants Trp, Asn, and Gly. The Arg-105 side chain rapidly shifts toward the entrance of the active site cavity, placing the charged group in direct contact with the solvent (results not shown). Consequently, the Arg side chain does not create the previously described physical barrier between BZ and Pro-107 in the same manner as the higher activity enzymes (Tyr, Trp, Asn). The resulting shift in the substrate is constrained by the presence of the long aliphatic side chain of Arg, which results in important steric interactions with the substrate molecule. Thus, a greater lateral movement of the BZ substrate is observed throughout the simulation, which may account for the 2.5-fold decrease observed in k_{cat}. In fact, the sulfur atom of the BZ thiazolidine ring in the Y105R mutant moves 2.65 Å from its original position during the 200-ps simulation relative to 0.36 Å for the wild-type complex. It should be noted that the Arg-105 side chain also shifts toward the entrance of the active site cavity in the absence of BZ, suggesting that solvation of the guanidinium group (rather than steric hindrance of the bound substrate) promotes this shift.

In the case of the Y105L mutant (Fig. 3*B*), the side chain of Leu is very flexible throughout the 200-ps trajectory (root mean square deviation = 1.35 Å as opposed to root mean square deviation values <0.8 Å for all other modeled mutants), possibly disrupting the efficient binding and stabilization of the substrate in the active site cavity. Similarly, we observed that the amide side chain of Gln is unable to adopt the parallel conformation shown for the aromatic and Asn mutants as a result of its greater length and flexibility (not shown). It is worth noting that both of these mutations (Leu and Gln) have a greater effect on the MIC values of cephalosporins than penicillins, suggesting that the bulkier dihydrothiazine ring of cephalosporin substrates does not support as much flexibility at position 105 than the thiazolidine ring of penicillin substrates. Taken with the poor MIC results of all other nonaromatic, branched mutations (with the exception of Asn), this suggests that a greater side-chain flexibility and size conferred by branched residues at position 105 have a detrimental effect on substrate binding. By conserving the planar conformation lined up against Pro-107, small or aromatic residues would

prevent steric interactions with the substrate by forming a stabilizing wall that restricts the active site cavity size and, thus, substrate movement.

Finally, by monitoring the dynamics trajectory of the Y105*X* mutants in the presence and absence of BZ, we determined that the whole-residue distance between residues 105 and 107 for aromatics (Tyr, Trp) is ~1 Å wider in the absence than in the presence of substrate. This difference is less pronounced (~0.5 Å) for the Asn mutant but is not discernible for three other mutants tested (Gly, Arg, Gln). The difference in distance (±substrate) appears to be correlated to *in vivo* and *in vitro* activity, further suggesting a role for residue 105 in substrate stabilization at the active site.

DISCUSSION

The results we have obtained indicate that the nature of the residue at position 105 in TEM-1 β-lactamase has an important effect on substrate recognition and stabilization at the active site. Stabilizing effects have been previously proposed for Tyr-105 with respect to substrates and inhibitors. Notably, Mobashery and co-workers (32, 33) suggest the existence of a hydrophobic pocket created by the side chains of Tyr-105 and Val-216 in TEM-1, whereas other studies on Class A enzymes pointed out that the hydroxyphenyl group of Tyr-105 was within van der Waals distance of the thiazolidine ring of penicillin substrates or inhibitors (9, 18, 34, 35). Consequently, these crystal structure observations have led to the suggestion that Tyr-105 "stacks" with the thiazolidine ring of BZ or inhibitors (21, 22). Our studies suggest that the strong bias for aromatic residues at position 105 is not a functional prerequisite of hydrophobicity so much as a structural necessity to prevent unfavorable substrate displacement within the active site. This hypothesis is strengthened by the polar Asn side chain of the Y105N mutant, whose activity is in the same range as the wild-type enzyme for all substrates tested. Thus, polarity can be tolerated at position 105 as long as the residue causes no perturbation to substrate positioning. Moreover, as evidenced by comparing the relatively high penicillin hydrolysis of the Y105G, Y105N, Y105S mutants with the more hydrophobic Y105C mutant, hydrophobicity cannot be considered as a variable defining the stabilizing interaction conferred by Tyr-105 in TEM-1 and other Class A β-lactamases.

Aromatic residues and Asn would, thus, be favored at position 105 because of the intrinsic planarity of their side chains, which enables them to adopt a structurally "non-destructive" conformation where they fill the small cavity between the thiol ring of the substrate on one side and Pro-107 on the other, preventing extensive motion of the substrate within the active site cavity. This wall, formed by Tyr-105, has previously been suggested as an important determinant in clavulanate susceptibility for several Class A enzymes (23), although this assertion needs more thorough investigation with respect to the susceptibility of Class A β-lactamases that do not harbor an aromatic residue at position 105. Because the Asp mutant would also be able to adopt the same planar conformation as that of Asn, it is reasonable to assume that the low *in vivo* and *in vitro* activities observed for Y105D with all the substrates tested is related to its negative charge. The presence of the wild-type glutamate residue at position 104 coupled to the Y105D mutation would generate a strong negative potential, which may account for the altered kinetic parameters. Finally, the side chains of other residues appear to be disfavored at position 105 as a result of their bulkier size, charge, and/or their inability to retain the particular non-destructive planar conformation described herein, which prevents unfavorable steric clashes of residue 105 with the substrate. Hence, small residues create a gap in this barrier, allowing for greater substrate displacement within the active site cavity, whereas larger and non-planar residues (except Asn) are too bulky and/or possess too many degrees of freedom to adopt this barrier conformation, interfering with productive substrate positioning. In the evolutionary context of this particular residue, our results are in accordance with the non-planar and bulky amino acids naturally excluded from this position, as their physical characteristics constitute a clear disadvantage with respect to catalytic efficiency, as opposed to the strongly conserved, structurally non-destructive residues (aromatics, Gly, Asn) found at position 105 in all Class A β-lactamases (Table II). As noted above, we were unable to select a Y105*X* mutation of TEM-1 that allowed recognition of a higher generation cephalosporin. That the conformation of residue 105 is not in the immediate vicinity of the bulky C7 side chain of third-generation cephalosporins (Fig. 1) suggests this residue may not be a primary target for future adaptive mutations found in natural isolates of TEM variants.

Although the planar characteristic conferred by aromatic residues and Asn at position 105 appears to be essential for efficient cephalosporin hydrolysis, it is not a definitive requirement of high activity for penicillin substrates since high survival rates are additionally observed for mutants with small amino acid side chains at position 105 (Y105G and Y105A). This observation suggests that cephalosporin stabilization in the active site of TEM-1 is more precarious and requires a greater structural integrity of the active site than penicillin substrates. This difference in recognition and stabilization may be attributed to the greater size of the 6-membered dihydrothiazine ring of cephalosporins coupled to the fact that these substrates always harbor a bulkier C3 substituent compared with the smaller, less substituted 5-membered thiazolidine ring of penicillins. Aromaticity, although not essential, may still contribute to affinity since the elimination of the aromatic moiety at position 105 results in K_m increases that could be explained by the loss of weak stabilizing forces conferred by aromatic residues. Accordingly, the lower K_m values observed toward BZ and CF for the Y105W mutant may result from the higher electron density of the Trp indole side chain compared with the hydroxyphenyl moiety of Tyr, resulting in stronger van der Waals contacts of the indole side chain with the substrate.

In the wild-type enzyme, ion-pairing interactions (36) and hydrogen bonding (37) of the C3 (C4) carboxylate group of substrates to the guanidinium group of Arg-244 have been suggested to play a role in stabilizing the substrate in the ground and transition states, although these assumptions have been the subject of debate (2, 4). Although our model of the acyl-enzyme intermediate cannot account for ground or transition states, the wild-type acyl-enzyme with BZ or CF supports this hypothesis by confirming the maintenance of appropriate distances between Arg-244 and the C3 (C4) carboxylic acid groups of both substrates throughout the 200-ps dynamics (shown in Fig. 4*A* for BZ). However, the large shift of the thiol rings of both BZ and CF observed for the Y105G mutant prevents any direct hydrogen bonding or ion-paring interaction of the C3 (C4) carboxylate moieties of substrates with Arg-244 as a result of increased distances (Fig. 4*B*). Should the increased distance also exist at the ground or transition states, this suggests either that interaction with Arg-244 is not essential for activity or that a bridging water molecule (as proposed by various authors (Ref. 4 and references therein)) would be displaced concurrently with the substrate, since the Y105G mutant is highly active for BZ hydrolysis.

We observed that the amide of Asn is positioned differently in the modeled, ligand-bound Y105N mutant and in the free-form crystal of the *M. fortuitum* enzyme. This suggests that the

position of residue 105 is different in the free and ligand-bound enzymes, possibly as a result of substrate binding. Our monitoring of the distance between residues 105 and 107 during the 200-ps dynamics trajectory of the Y105*X* mutants modeled in the presence and absence of BZ supports this hypothesis. The correlation between the difference in distance (±substrate) and *in vivo* and *in vitro* activity suggests that aromatic residues at position 105 (and Asn to a certain extent) adopt two distinct conformations in the presence and absence of substrate and could, thus, be a determinant of recognition for substrate stabilization. This conformational change is in agreement with backbone NMR relaxation studies of TEM-1 showing that residue 105 harbors a higher-than-average flexibility in solution.[2] Moreover, previously published crystal structures of inhibitor-bound Class A β-lactamases showed Tyr-105 as a potentially flexible residue harboring distinct positions in the free and inhibitor-bound enzymes (17–21). Recently, a 1-ns molecular dynamics simulation of TEM-1 with BZ showed that the side chain of Tyr-105 can flip in the same plane to make favorable contacts with the phenyl moiety of this substrate (12). Although the side chain of Tyr-105 does not display this important conformational shift in our shorter modeling studies of TEM-1, our results nevertheless suggest that Tyr-105 as well as highly active Y105*X* mutations adopt slightly differing conformations in the presence and in absence of substrate.

In conclusion, our systematic investigation of the *in vivo* and *in vitro* kinetic effects of Y105*X* mutants of TEM-1 β-lactamase coupled to molecular dynamics simulations identify this residue as being involved in β-lactam substrate selectivity and stabilization at the active site. We propose that the residue at position 105 is most propitious to substrate binding when it can stably adopt a planar conformation between the substrate and the conserved Pro-107, whereas more flexible residues create unfavorable steric hindrance with the substrate. Polarity (but not charge) is tolerated, whereas reduction of bulk at this position results in discrimination between penicillin and first-generation cephalosporin substrates. We obtain good agreement between *in vivo*, *in vitro*, and *in silico* results, which also correlate well with the natural diversity observed at this position among Class A β-lactamases, thus suggesting a basis for the evolutionary selection of residues adopting a non-destructive conformation at position 105 in Class A β-lactamases.

Acknowledgments—We are grateful to Prof. Natalie C. J. Strynadka (University of British Columbia, Vancouver, BC) and Pierre-Yves Savard and Prof. Stéphane M. Gagné (Université Laval, Québec, QC) for helpful discussions. We also thank Peter D. Pawelek (McGill University, Montréal, QC) and Roberto A. Chica and Prof. Jeffrey W. Keillor (Université de Montréal, Montréal, QC) for careful reading of the manuscript.

REFERENCES

1. Orencia, M. C., Yoon, J. S., Ness, J. E., Stemmer, W. P., and Stevens, R. C. (2001) *Nat. Struct. Biol.* **8,** 238–242
2. Matagne, A., and Frère, J. M. (1995) *Biochim. Biophys. Acta* **1246,** 109–127
3. Matagne, A., Lamotte-Brasseur, J., and Frère, J. M. (1998) *Biochem. J.* **330,** 581–598
4. Knox, J. R. (1995) *Antimicrob. Agents Chemother.* **39,** 2593–2601
5. Yang, Y., Rasmussen, B. A., and Shlaes, D. M. (1999) *Pharmacol. Ther.* **83,** 141–151
6. Minasov, G., Wang, X., and Shoichet, B. K. (2002) *J. Am. Chem. Soc.* **124,** 5333–5340
7. Chen, C. C., and Herzberg, O. (2001) *Biochemistry* **40,** 2351–2358
8. Strynadka, N. C. J., Adachi, H., Jensen, S. E., Johns, K., Sielecki, A., Betzel, C., Sutoh, K., and James, M. N. G. (1992) *Nature* **359,** 700–705
9. Tranier, S., Bouthors, A. T., Maveyraud, L., Guillet, V., Sougakoff, W., and Samama, J. P. (2000) *J. Biol. Chem.* **275,** 28075–28082
10. Shimamura, T., Ibuka, A., Fushinobu, S., Wakagi, T., Ishiguro, M., Ishii, Y., and Matsuzawa, H. (2002) *J. Biol. Chem.* **277,** 46601–46608
11. Meroueh, S. O., Roblin, P., Golemi, D., Maveyraud, L., Vakulenko, S. B., Zhang, Y., Samama, J. P., and Mobashery, S. (2002) *J. Am. Chem. Soc.* **124,** 9422–9430
12. Díaz, N., Sordo, T. L., Merz, K. M., Jr., and Suárez, D. (2003) *J. Am. Chem. Soc.* **125,** 672–684
13. Castillo, R., Silla, E., and Tuñón, I. (2002) *J. Am. Chem. Soc.* **124,** 1809–1816
14. Abraham, E. P., and Chain, E. (1940) *Nature* **146,** 837
15. Escobar, W. A., Miller, J., and Fink, A. L. (1994) *Biochem. J.* **303,** 555–558
16. Di Gleria, K., Halliwell, C. M., Jacob, C., and Hill, H. A. (1997) *FEBS Lett.* **400,** 155–157
17. Chen, C. C., Rahil, J., Pratt, R. F., and Herzberg, O. (1993) *J. Mol. Biol.* **234,** 165–178
18. Guo, F., Huynh, J., Dmitrienko, G. I., Viswanatha, T., and Clarke, A. J. (1999) *Biochim. Biophys. Acta* **1431,** 132–147
19. Wang, X., Minasov, G., Blázquez, J., Caselli, E., Prati, F., and Shoichet, B. K. (2003) *Biochemistry* **42,** 8434–8444
20. Maveyraud, L., Mourey, L., Kotra, L. P., Pedelacq, J. D., Guillet, V., Mobashery, S., and Samama, J. P. (1998) *J. Am. Chem. Soc.* **120,** 9748–9752
21. Strynadka, N. C. J., Martin, R., Jensen, S. E., Gold, M., and Jones, J. B. (1996) *Nat. Struct. Biol.* **3,** 688–695
22. Strynadka, N. C. J., Jensen, S. E., Alzari, P. M., and James, M. N. G. (1996) *Nat. Struct. Biol.* **3,** 290–297
23. Page, M. G. F. (2000) *Drug Resist. Updat.* **3,** 109–125
24. Huang, W. Z., Petrosino, J., Hirsch, M., Shenkin, P. S., and Palzkill, T. (1996) *J. Mol. Biol.* **258,** 688–703
25. Ho, S. N., Hunt, H. D., Horton, R. M., Pullen, J. K., and Pease, L. R. (1989) *Gene* (*Amst.*) **77,** 51–59
26. Cantu, C., III, Huang, W., and Palzkill, T. (1996) *J. Biol. Chem.* **271,** 22538–22545
27. Bouthors, A. T., Dagoneau-Blanchard, N., Naas, T., Nordmann, P., Jarlier, V., and Sougakoff, W. (1998) *Biochem. J.* **330,** 1443–1449
28. Jelsch, C., Mourey, L., Masson, J. M., and Samama, J. P. (1993) *Proteins* **16,** 364–383
29. Bush, K., and Mobashery, S. (1998) *Adv. Exp. Med. Biol.* **456,** 71–98
30. Page, M. I. (1987) *Adv. Phys. Org. Chem.* **23,** 165–270
31. Wolozin, B. L., Myerowitz, R., and Pratt, R. F. (1982) *Biochim. Biophys. Acta* **701,** 153–163
32. Taibi-Tronche, P., Massova, I., Vakulenko, S. B., Lerner, S. A., and Mobashery, S. (1996) *J. Am. Chem. Soc.* **118,** 7441–7448
33. Bulychev, A., Obrien, M. E., Massova, I., Teng, M., Gibson, T. A., Miller, M. J., and Mobashery, S. (1995) *J. Am. Chem. Soc.* **117,** 5938–5943
34. Maveyraud, L., Massova, I., Birck, C., Miyashita, K., Samama, J. P., and Mobashery, S. (1996) *J. Am. Chem. Soc.* **118,** 7435–7440
35. Ness, S., Martin, R., Kindler, A. M., Paetzel, M., Gold, M., Jensen, S. E., Jones, J. B., and Strynadka, N. C. (2000) *Biochemistry* **39,** 5312–5321
36. Moews, P. C., Knox, J. R., Dideberg, O., Charlier, P., and Frère, J. M. (1990) *Proteins* **7,** 156–171
37. Zafaralla, G., Manavathu, E. K., Lerner, S. A., and Mobashery, S. (1992) *Biochemistry* **31,** 3847–3852
38. Dideberg, O., Charlier, P., Wery, J. P., Dehottay, P., Dusart, J., Erpicum, T., Frère, J. M., and Ghuysen, J. M. (1987) *Biochem. J.* **245,** 911–913
39. Swarén, P., Maveyraud, L., Raquet, X., Cabantous, S., Duez, C., Pedelacq, J. D., Mariotte-Boyer, S., Mourey, L., Labia, R., Nicolas-Chanoine, M. H., Nordmann, P., Frère, J. M., and Samama, J. P. (1998) *J. Biol. Chem.* **273,** 26714–26721
40. Ambler, R. P., Coulson, A. F., Frère, J. M., Ghuysen, J. M., Joris, B., Forsman, M., Levesque, R. C., Tiraby, G., and Waley, S. G. (1991) *Biochem. J.* **276,** 269–270

[2] P.-Y. Savard and S. M. Gagné, Université Laval, Québec, QC, personal communication.